Int. J. Electrochem. Sci., 12 **(2017)** 1004 – 1013, doi: 10.20964/2017.02.48

International Journal of ELECTROCHEMICAL SCIENCE
www.electrochemsci.org

Short Communication

Lithium Intercalation into Graphene Ribbons of Glassy Carbon

Yun Wu[1], *Takeyoshi Okajima*[1] *and Takeo Ohsaka* [1,2,*]

[1] Department of Electronic Chemistry, Interdisciplinary Graduate School of Science and Engineering, Tokyo Institute of Technology, 4259-G1-5, Nagatsuta, Midori-ku, Yokohama 226-8502, Japan
[2] Present Address: Research Institute for Engineering, Kanagawa University, 3-27-1 Rokkakubashi, Kanagawa-Ku, Yokahama 221-8686, Japan
[*]E-mail: ohsaka@echem.titech.ac.jp, pt120866sa@kanagawa-u.ac.jp

Received: 7 November 2016 / *Accepted:* 22 December 2016 / *Published:* 30 December 2016

The lithium intercalation into a glassy carbon (GC) electrode, which is a partially graphitized carbon with a turbostratic structure, during the electrodeposition of lithium at the GC electrode in propylene carbonate (PC) solution containing 0.1 M $LiClO_4$ and the lithium deintercalation from the GC electrode were investigated by X-ray photoelectron spectroscopy (XPS), X-ray diffraction (XRD) technique and cyclic voltammetry (CV). The formation of lithium graphite intercalation compounds (LiC_{6n}) was confirmed by XPS and XRD measurements. The (002) Bragg peak for the Li-electrodeposited GC powder shifted to a smaller scattering angle (2θ) compared with that for the GC powder, i.e., 2θ = 25.1 and 21.2º which gave the interlayer spacing (d) of 3.54 and 4.19 Å, respectively, for the GC and Li-electrodeposited GC powders, giving a direct evidence of the lithium intercalation into graphene ribbons of the GC. The lithium intercalation / deintercalation behavior was considered to be reflected on the CVs obtained for the reduction / oxidation process observed at the GC electrode. Based on the results obtained, it was also suggested that the insertion / deinsertion to / from the cavities such as microvoids (pores) of the GC electrode substrate may take place along with the lithium intercalation / deintercalation into / from the graphene ribbon layers.

Keywords: Lithium electrodeposition; Intercalation; Glassy carbon; Graphene ribbon

1. INTRODUCTION

Glassy carbon (GC) was prepared by Yamada and Sato in 1962[1] and owing to its physical and chemical properties it has become an interesting and widely applied electrode material for more than half a century[2-5]. It exhibits an excellent electric conductivity, a rather low oxidation rate and a rather high chemical inertness which, together with very small pores and a small gas and liquid permeability, make GC a conventional inert electrode[3,4]. GC is a partially graphitized carbon with a

trubostratic structure and has a relatively low density (1.45) due to its graphite-like ribbons containing micro-pores, compared with 2.2 in single crystals of graphite[2].

The intercalation of lithium ions into graphite has been extensively studied because graphite intercalation compounds with lithium ions as intercalates have been used for commercial applications as active anode materials for lithium-ion cells[6]. Compared to it, only a little work has been carried out on lithium intercalation into GC. Halpin and Jenkins[7] examined the interaction of GC with potassium and sodium metal vapor using X-ray diffraction techniques and mentioned that intercalation by alkali metals is possible in all carbons and disrupts aggregates of non-graphitizing carbons. Guerard and Herold reported that lithium intercalates into graphite and other carbons including soft and hard carbons[8]. Skowronski and Knofczynski[9] examined the uptake of lithium ions by the GC spheres which were prepared from phenolic resin in nitrogen atmosphere and reported that after the heat treatment in argon atmosphere at 2700 ℃ the uptake of lithium ions occurs via the insertion / deinsertion mechanism characteristic of hard carbon due to lack of long-range stacks of graphene layers, while after the heat treatment at 1000℃ under ambient pressure using iron powder as catalyst, the intercalation / deintercalation characteristic of graphite predominates. In the former case, the GC is a non-graphitizable, turbostratic carbon having nanopores into which lithium ions are inserted. On the other hand, in the latter case, the GC contains the graphite phase admixed with turbostratic carbon.

High-resolution electron micrograph of GC indicates that the network consists of long and narrow stacked graphite-like ribbons randomly oriented[2,10]. Thus, lithium can be considered to intercalate into graphene ribbons of GC. In the present study, in order to clarify whether lithium intercalates into stacked graphene ribbon layers of GC, the electro-deposition of lithium was performed on a GC electrode in propylene carbonate(PC) containing 0.1 M $LiClO_4$. The electro-deposition led to the change of the color of the electrode surface from black before the lithium deposition to steel-blue and brass-yellow, which are characteristic colors of lamellar graphite-lithium compounds, after the deposition. This observation suggested the formation of lithium intercalation carbon compounds during the lithium electro-deposition. We further characterized the obtained electrode by X-ray photoelectron spectroscopy (XPS), which proved that lithium intercalation compound LiC_{6n} was formed in the GC electrode. X-ray diffraction (XRD) pattern measurements provided a direct evidence for lithium intercalation into the GC electrode. In addition, the intercalation / deintercalation process was also examined by cyclic voltammetry.

2. EXPERIMENTAL

2.1 Reagents

GC electrodes (disk) and GC powder made at 2000 °C were obtained from Tokai Carbon Co., Ltd. Propylene carbonate (PC) of reagent grade was purchased from Kanto Chemicals Co., Inc. 0.5 mol / L H_2SO_4 solution and anhydrous lithium perchlorate ($LiClO_4$) of reagent grade were purchased from Wako Pure Chemical Industries, Ltd. All the chemicals were used as received without further purification.

2.2 Pretreatment of electrodes

GC electrode was polished first with sandpaper (No. 600 and No. 2000) and then with alumina powder (in the order of 1.0 and 0.06 μm). Residual alumina on the GC electrode surface was rinsed out with Milli-Q water and subsequently washed ultrasonically in Milli-Q water for 15 min. Electrochemical pretreatment was performed by repeating the potential scan at 0.1 V s^{-1} between -0.2 and 1.4 V vs. silver/silver chloride electrode (Ag/AgCl/KCl sat.) in deoxygenated 0.5 M H_2SO_4.

2.3 Preparation of GC-Li electrode by a constant - current electrolysis

The electrodeposition of lithium was performed in a three-electrode electrochemical cell system at 25 °C. GC disk (diameter: 6 mm) was used as the working electrode while a GC plate (2.5 cm^2) and a silver wire were used as counter and quasi-reference electrodes, respectively. To prevent the contamination from water and oxygen, the electrodeposition was conducted in an Ar gas-filled glove box. For the electrodeposition of lithium a constant current density of -0.5 mA cm^{-2} was applied on the GC disk in PC (10 mL) containing 0.1 M $LiClO_4$ via a 2000–50 V galvanostat connected with a 3320 G coulometer (Toho Technical Co. Ltd., Japan). After an arbitrary amount of charge (10 C cm^{-2}) was passed, the electrodeposition was stopped and the thus-obtained electrode was denoted as GC-Li (10 C cm^{-2})[11]. The obtained electrode was dried in vacuum oven at 100 °C for 10 h and subsequently characterized by X-ray photoelectron spectroscopy (XPS). For XPS measurements, the GC-Li electrode was placed under an ultra-high vacuum condition (1× 10^{-6} Pa) where an ESCA-3400 electron spectrometer (SHIMADZU) with unmonochromatized X-ray source [Mg Kα (hυ = 1,253.6 eV) anode, emission current of 20 mA and acceleration voltage of 10 kV] was employed, operating at 200 W. The photoelectron take-off angle was set to 75°, and the analyzer pass energy was set to 75 eV. The binding energies of different elements were referred to NIST X-ray Photoelectron Spectroscopy Database[12]. The etching process was performed using an argon ion beam (accelerating voltage 2 keV, ion beam vurrent 7-8 μA). To take insight of the depth profile of each element, the etching was performed by using 1.5 keV Ar^+ ion to sputter the surface for a time of 15 and 30 min, with a 5 × 10^{-4} Pa Ar gas atmosphere. The etching rate was calculated to be 4 Å / min.

2.4 GC-Li powder (40 C cm^{-2}) for XRD characterization

150 mg GC powder was weighed into a 2 mL tube followed by the addition of 1 mL DMF and 0.15 mL Nafion solution (5 wt %, Sigma). The mixture was sonicated in ice-cold water bath for 3 h. The GC plate (two sides, one side: 1 cm^2) was modified with 100 μL of the mixture solution (50 μL / side). The electrode was then dried at room temperature and applied to conduct lithium electrodeposition in 0.1 M $LiClO_4$ solution (100 mL) with a constant-current density of -0.5 mA cm^{-2} applied. After 40 C cm^{-2} was passed, the electrode was taken out and dried in vacuum oven at 100 °C for 10 h. Finally, the GC-Li powder (40 C cm^{-2}) was detached from the GC plate and grinded to uniform powder in Ar-filled glove box. The GC-Li powder was sealed in a quartz capillary with a

diameter of 0.3 mm for the X-ray diffraction (XRD) characterization. Diffraction data was collected from 10° to 90° in a step of 0.01° (Rigaku, SmartLab and Ultima).

The lateral size (L_a) and the stacking height (L_c) of the crystallite were determined using the following Scherrer equations (1) and (2)[13]

$L_a = 1.84\lambda/B_a \cos\varphi_a$ (1)

and

$L_c = 0.89\lambda/B_c \cos\varphi_c$ (2)

where the λ is the wavelength of X-ray (1.5406 Å), B_a and B_c are the full width at half maximum (FWHM) of the (100) and (002) peaks of GC lattice and φ_a and φ_c are the corresponding scattering angles or peak positions. The FWHM values of the (100) and (002) peaks were analyzed by OriginPro 8.

2.5 Electrochemical behavior of GC-Li electrode

A CHI electrochemical analyzer 750B (BAS Inc., Japan) was used to perform cyclic voltammetry. Electrochemical characterizations were done in 0.5 M H_2SO_4 solution or PC solution containing 1.0 M $LiClO_4$ with a three-electrode system at room temperature (25 °C).

3. RESULTS AND DISCUSSION

Fig. 1 shows the C 1s and Li 1s XPS profiles of the As-prepared GC-Li (10 C cm^{-2}) and the GC-Li (10 C cm^{-2}) after the etching of 15 and 30 min using an Argon ion beam. Each spectrum was deconvoluted to the carbon and lithium of the species (or functional groups) indicated in each figure. As for the as-prepared GC-Li (10 C cm^{-2}), the peak around 286 eV was deconvoluted to several peaks corresponding to phenolic and carbonyl carbons, lithium alkyl carbonate (RCH_2CO_3Li) and lithium graphite intercalation compounds (LiC_{6n}). It is reported previously that lithium alkyl carbonates are formed as a result of the electrolyte decomposition during the lithium intercalation process in 1 M $LiClO_4$ PC/PE (50 / 50) electrolyte[14]. After the lithium electrodeposition, we found that the GC electrode surface indicates various colors partially, which are obviously different from its original color (i.e. black), i.e., mainly steel-blue and brass-yellow, suggesting the coexistence of lithium intercalation compounds in different stages[8]. The binding energy of LiC_6 is reported to be 285.2 eV[15]. However, it was impossible to verify which stages in LiC_{6n} were obtained actually, because no binding energies for the second, third and fourth stages are available in literature and XPS database. The peak around 291 – 292 eV was deconvoluted to Li_2CO_3 and lithium alkyl carbonate (RCO_3Li) and that at 293 eV is considered to correspond to phenolic ether[16]. As for the Li region, the peak at 56.3 eV was deconvoluted to Li_2CO_3 / RCO_3Li, LiCl (and LiOH) and LiC_{6n}. LiCl is formed by the chemical reaction between electrodeposited Li metal and ClO_4^- [17] and LiOH is the product of the reaction of LiC_{6n} with H_2O[8] in the atmosphere during the sample preparation process for XPS measurements. The peak at 56.3 is assigned to Li_2CO_3 and also to RCO_3Li because of similar chemical bonding environments of Li in both compounds.

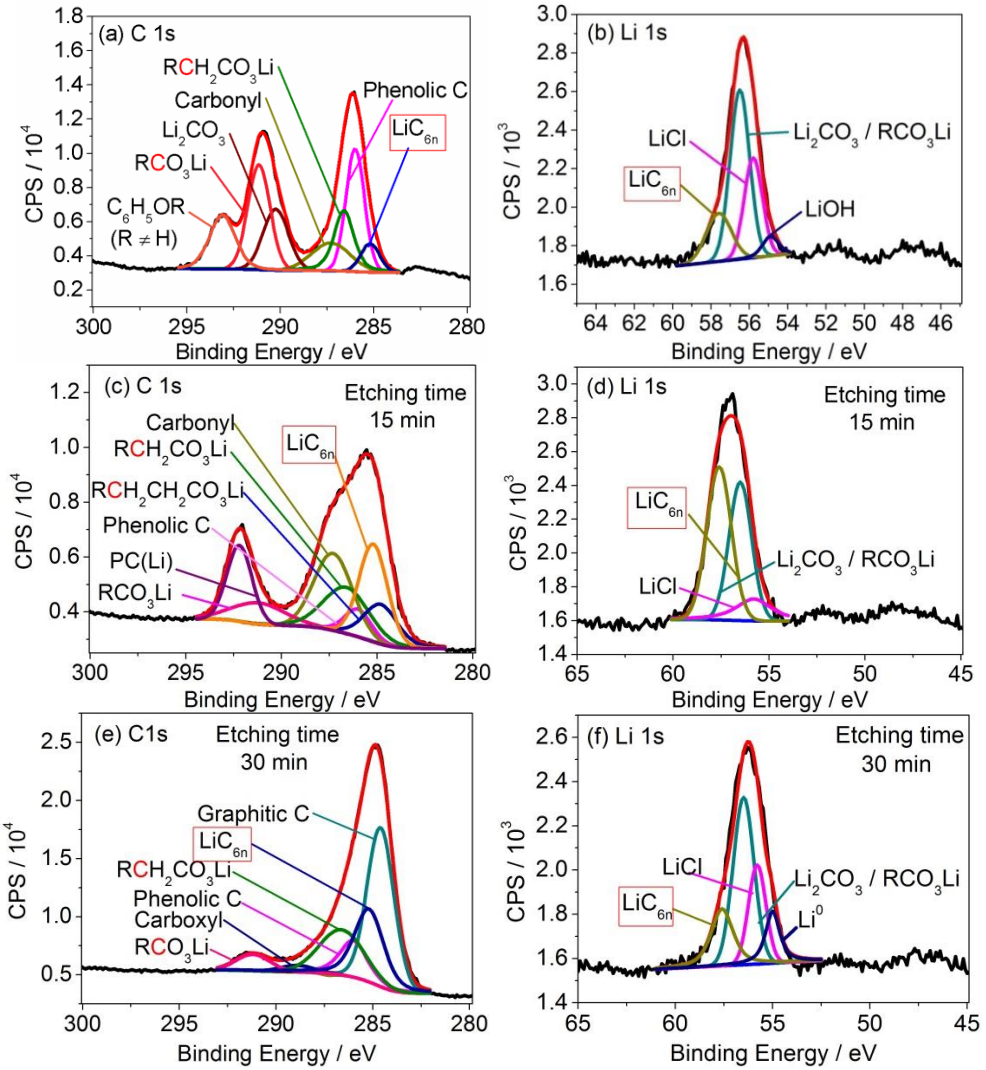

Figure 1. High-resolution C 1s and Li 1s XPS spectra of (a, b) as-prepared GC-Li (10 C cm^{-2}) and after etching for 15 min (c, d) and 30 min (e, f). Each spectrum is deconvoluted to carbon and lithium of the species indicated in each figure and the overall fitting is shown by a red line.

After the etching of 15 min, the intensity of carbon decreased while that of lithium increased, as compared with that before the etching (Fig. 1(c and d)). The peak of LiC_{6n} is larger than that before the etching, which means that the content of LiC_{6n} is higher after the etching. The fitted peak PC(Li) was observed, indicating that PC solvent could also co-intercalate into the GC electrode and its accommodation sites are the crystal boundary of GC[18]. After the etching of 30 min, the peak corresponding to graphitic carbon appeared clearly while the peak of RCO_3Li became small. As shown in Fig. 1(f), the peak ascribable to lithium metal was observed showing that some lithium element exists in the form of atom. As reported[19-21], when lithium inserts into hard carbon materials, lithium exists between graphene layers, in the pores, and at the edge of graphene and also is absorbed in both sides of single graphene layers. When lithium exists between graphene layers, 0.72 e is transferred from lithium to the antibonding orbital of graphene indicating the atomic quality[22], and thus the lithium is partially charged positively. When lithium exists in the pores, at the edge of graphene or is

absorbed on both sides of single carbon layer, it exhibits the quality of atom. Consequently, lithium metal was observed by the XPS measurement. As seen from the cyclic voltammograms (CVs) obtained at the GC-Li (10 C cm^{-2}) in 0.5 M H_2SO_4 solution (Fig. 2), the anodic current corresponding to the oxidation of the Li metal intercalated (and inserted) into the GC substrate to Li^+ ion was observed continuously during both the forward and backward potential scans (20 repeative CVs are shown here). The detailed analysis of the cyclic voltammetric behavior of the Li-electrodeposited GC electrode in aqueous solutions will be reported elsewhere.

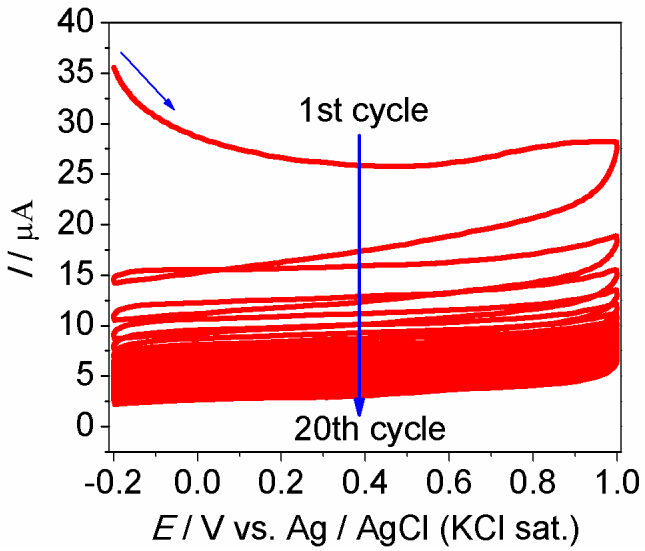

Figure 2. Cyclic voltammograms (20 cycles) continuously recorded of GC-Li (10 C cm^{-2}) at 10 mV s^{-1} in 0.5 M H_2SO_4 solution.

It is well-known that GC is a partially graphitized form of carbon and have a turbostratic structure, i.e., it is composed of graphite-like microcrystallites[23,24]. Consequently, when lithium is intercalated into GC, lithium graphite intercalation compounds are formed. As shown by the XPS characterization, lithium-containing compounds such as Li_2CO_3, and RCO_3Li result from the solid-electrolyte interface (SEI) formation via electrolyte decomposition on the surface of GC electrode[25]. Thus, by removing SEI layer, lithium graphite intercalation compounds were detected (Fig. 1(f)).

The atomic ratios of C and Li for the GC-Li (10 C cm^{-2}) before and after the Ar^+ ion etching were calculated using the atomic sensitivity factors of both elements: C (1s) and Li (1s) are 0.25 and 0.02, respectively[26] (Table 1). At a glance, we can see that the atomic ratios of N(C) / N(Li) are much larger than that (e.g., 6 / 1 for LiC_6) expected for LiC_{6n}. This fact together with the structural model[2] and TEM image of GC (Fig. 3) may suggest that Li is intercalated into the stacking graphene ribbons[20,21] as well as absorbed on both sides of graphene ribbons and / or inserted into some cavities such as microvoids, cluster gaps and atomic defects[19].

Table 1. Atomic ratios of Li and C of GC-Li (10 C cm^{-2}) before and after the Ar^+ ion etching

Etching time / min	N(C) / N(Li)
0	1.45 / 1
15	0.85 / 1
30	1.63 / 1

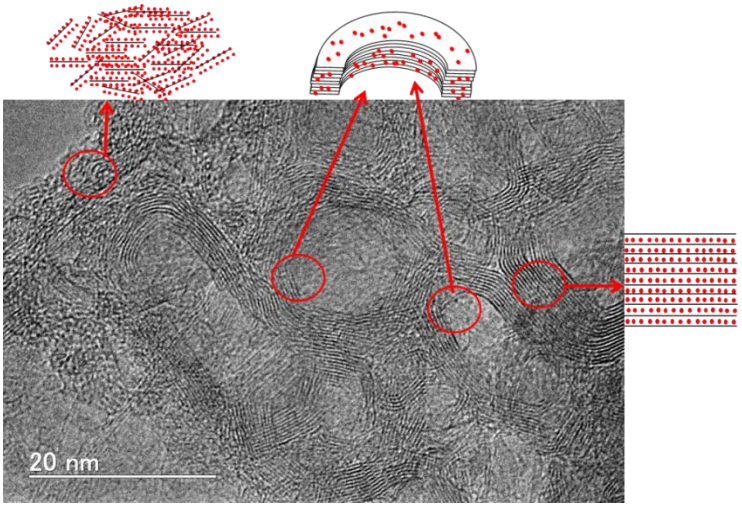

Figure 3. TEM image of GC and probable accommodation sites of lithium.

XRD characterization was employed to further confirm the formation of lithium graphite intercalation compound during the Li electrodeposition at the GC electrode and the result is shown in Fig. 4. The XRD pattern of the GC shows three broad peaks at scattering angle 2θ = 25.1, 43.3 and 78.8º, which can be assigned to (002), (100) and (110) indices, respectively, of the GC lattice[23]. The (100) and (110) peaks are obviously asymmetric, indicating that GC has a turbostratic structure: within a domain, each graphene layer is oriented at random relative to its neighbours ribbons. The lateral extent of graphene ribbons can be estimated from the FWHM of (100) diffraction peak[27]. At 2θ = 43.3º, the FWHM is 3.8º, from which L_a is calculated to be 46.0 Å. The GC exhibits a relatively weak (002) Bragg peak compared with graphite[28]. This weak and wide (002) peak results from the diffraction of parallel stacking graphene ribbons. This result is in agreement with the TEM data shown in Fig. 3. The number of graphene ribbons stacking in parallel and the spacing d between these ribbons could be estimated through the width of (002) diffraction peak[29,30]: At 2θ = 25.1º, the FWHM is 8.0º, through which L_c is calculated to be 10.1 Å. It is also obvious from the comparison of the XRD patters of the GC and GC-Li (40 C m^{-2}) that the diffraction peak from (002) plane for the GC-Li (40 C cm^{-2}) is shifted to a smaller value of 2θ compared with that of the GC, i.e., in the case of the GC the (002) peak locates at 2θ = 25.1º and after the lithium electrodeposition it is observed at 2θ = 21.2º. According to the Bragg's equation, the values of the interlayer spacing d between (002) lattice planes are calculated to be 3.54 and 4.19 Å for the GC and GC-Li (40 C cm^{-2}), respectively. This observed shift of the (002) Bragg peak is a direct evidence supporting the intercalation of lithium to graphene

ribbons of the GC substrate during the lithium electrodeposition at the GC electrode. Combined with the results of XPS, we could conclude that lithium could intercalate into graphene ribbons of GC in the form of lithium graphite intercalation compounds.

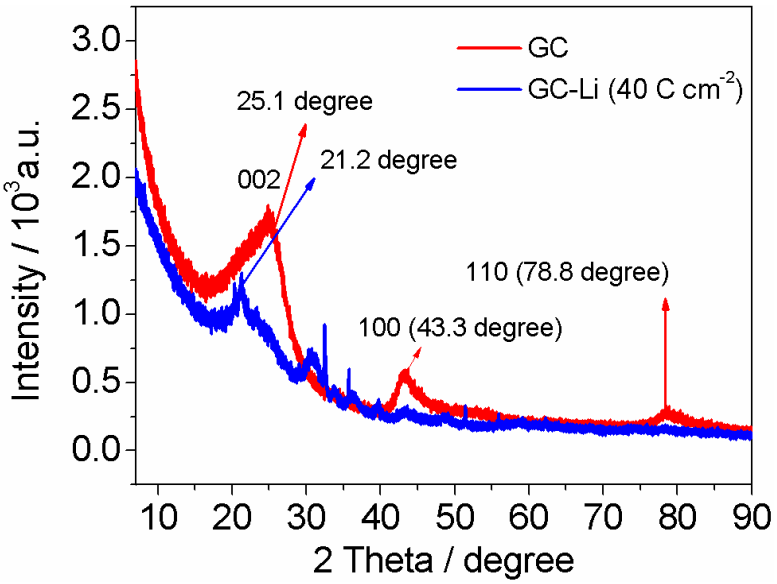

Figure 4. XRD patterns of GC-Li (40 C cm^{-2}) and GC powders.

Fig. 5(a) shows the typical CVs obtained at the GC electrode in PC solution containing 1.0 M $LiClO_4$ at various potential scan rates. The reduction and the oxidation currents were observed clearly. Interestingly, a larger reduction (oxidation) current was obtained at slower scan rate, which is completely different from the CV behavior expected for the redox reaction of the Li^+ / Li couple, i.e., the deposition – dissolution of lithium. The CVs indicating the electrochemical deposition – dissolution of lithium are given in Fig. 5(b) in which Ni electrode is used as the working electrode because a simple deposition – dissolution of the Li^+ / Li couple has been known to take place at this electrode[31]. In this case, as expected, both the cathodic and anodic currents increase with increasing the potential scan rate. In addition to the different potential scan rate dependences of the CVs at the GC and Ni electrodes, we can also see that the current density at the GC electrode is much smaller than that at the Ni electrode, indicating that the overall electrode reaction at the GC electrode is slower that at the Ni electrode. In both cases, the overall reaction rate (i,e., current) is controlled by the slowest step in the individual reactions. Therefore, the overall reaction at the GC electrode may be controlled by the other process(es) rather than the electrode reaction itself (electron transfer step) and the diffusion of Li^+ ion in the PC solution. By taking the above-mentioned results into account, the Li intercalation (and insertion) / Li deintercalation (and deinsertion) can be considered to be reflected on the observed CV behavior at the GC electrode. The Li intercalation / deintercalation to / from graphite layers is much slower that the diffusion of Li^+ ion in solution[32]. The detailed analysis of the CV behavior obtained for the lithium electrodeposition at the GC electrode is now in progress.

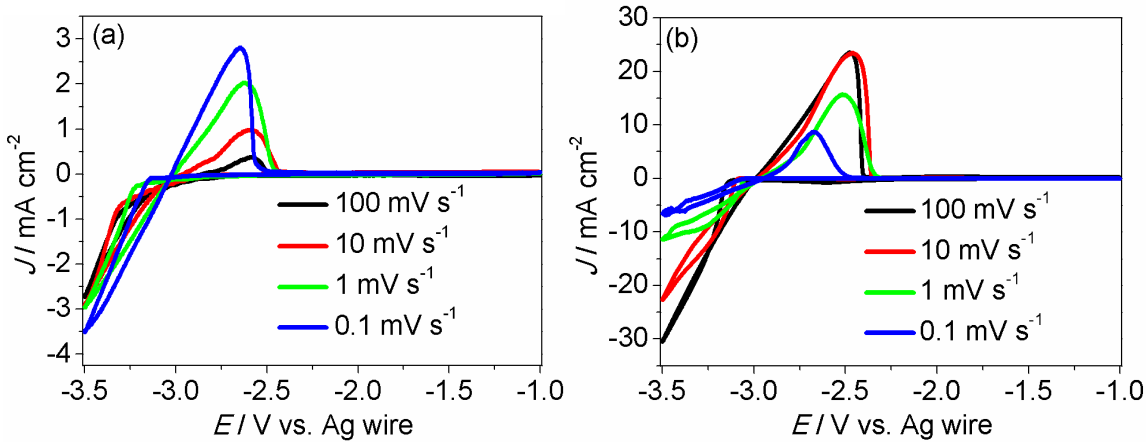

Figure 5. Cyclic voltammograms obtained at (a) GC and (b) Ni electrodes in PC solution containing 1.0 M $LiClO_4$ at various potential scan rates in Ar-filled dry glove box.

4. CONCLUSIONS

It was confirmed by XPS, XRD and CV that both the lithium intercalation into graphene ribbons of the GC electrode substrate during the lithium electrodeposition in PC solution containing 0.1 M $LiClO_4$ and the lithium deintercalation during the corresponding oxidation process take place. The shift of the (002) Bragg peak to a smaller value of 2θ for the lithium – electrodeposited GC powder companied with that for the GC powder provided a direct evidence of the lithium intercalation into graphene ribbons of the GC which are stacked in parallel. The formation of Li graphite intercalation compounds, LiC_{6n}, was also confirmed by the XPS measurements. CV was used to characterize the lithium intercalation / deintercalation process. In addition, the results obtained suggested that the insertion / deinsertion to / from the cavities such as microvoids of the GC electrode substrate may occur along with the lithium intercalation / deintercaltion.

ACKNOWLEDGEMENTS
The present work was financially supported by the Ministry of Education, Culture, Sports, Science and Technology (MEXT), Japan. The authors are grateful to Dr. Guowei Zhao, Yulong Sun and Professor Ryoji Kano at Tokyo Institute of Technology (TIT) for their help in XRD measurements. The authors thank Professor Fusao Kitamura at TIT for helpful discussion. Y. W. also greatly acknowledges MEXT and CSC (China Scholarship Council) for scholarships.

References

1. S. Yamada, H. Sato, *Nature*, 193 (1962) 26.
2. G. M. Jenkins, K. Kawamura, *Nature*, 231 (1971) 175.
3. G. N. Kamau, *Anal. Chim. Acta*, 207 (1988) 1.
4. A. Dekanski, J. Stevanovic, R. Stevanovic, B. Z. Nikolic, V. M. Jovanovic, *Carbon*, 39(2001) 1195.
5. C. Julien, Z. Stoynov, *Materials for lithium-ion batteries*, Springer Science & Business Media

(2000) Overijse, Belgium.
6. M. K. Halpin, G. M. Jenkins, *Pro. Roy. Soc. Lond. A*, 313 (1969) 421.
7. D. Guerard, A. Herold, *Carbon*,13 (1975) 337.
8. J. M. Skowronki, K.Knofczynski, *J. New Mat.Electrochem. Systems*, 9 (2006)359.
9. P. J. F. Harris, *Phil. Mag.*, 84 (2004) 3159.
10. Z. Awaludin, M. Suzuki, J. Masud, T. Okajima, T. Ohsaka, *J. Phys. Chem. C*, 115 (2011) 25557.
11. https://srdata.nist.gov/xps/Default.aspx.
12. B. Manoj, A. G. Kunjomana, *Int. J. Electrochem. Sci.*, 7 **(**2012**)** 3127
13. Z. X. Shu, R. S. McMillan, J. J. Murray, *J. Electrochem. Soc.*, 140 (1993) 922.
14. G. K. Wertheim, P. M. T. Van Attekum, S. Basu, *Solid State Commun*, 33 (1980) 1127.
15. G. Ilangovan, K. Chandrasekara Pillai, *Langmuir*, 13 (1997) 566.
16. K. I. Morigaki, A. Ohta, *J. power sources, 76* (1998) 159-166.
17. H. L. Zhang, C. H. Sun, F. Li, C. Liu, J. Tan, H. M. Cheng, *J. Phys. Chem. C*, 111 (2007) 4740.
18. M. Winter, J. O. Besenhard, M. E. Spahr, P. Novak, *Adv. Mater.*, 10(1998)725.
19. J. R. Dahn, T. Zheng, Y. Liu, J. S. Xue, *Science*, 270 (1995) 590.
20. K. Sato, M. Noguchi, A. Demachi, N. Oki, M. Endo, *Science*, 264 (1994) 556.
21. M, Khantha, N. A. Cordero, L. M. Molina, J. A. Alonso, L. A. Girifalco, *Phys. Rev. B*, 70 (2004) 125422.
22. S.S. Bukalov, L. a Leites, I. Sorokin, S. Kotosonov, *Nanosyst. Physics Chem. Math.*, 5 (2014) 186.
23. Y. Hishiyama, M. Nakamura, *Carbon*, 33 (1995) 1399.
24. K. Kanamura, S. Shiraishi, H. Tadezawa, Z. Takehara, *Chem. Mater.*, 9(1997)1797.
25. C. Wagner, D. Briggs, M. Seah, Practical surface analysis: Auger and X-ray Photoelectron
26. Spectroscopy 1(1990) 595
27. T. Noda, M. Inagaki, *Bull. Chem. Soc. Jpn.*, 37 (1964) 1534.
28. Z. Li, C. Lu, Z. Xia, Y. Zhou, Z. Luo, *Carbon*, 45 (2007) 1686.
29. W. Xing, J. Xue, T. Zheng, A. Gibaud, J. Dahn, *J. Electrochem. Soc.*, 143(1996) 3482.
30. B. E. Warren, Phys. Rev., 59 (1941) 693.
31. R. Wibowo, S. E. W. Jones, R. G. J. Compton, *Chem. Eng. Data*, 55 (2010) 1374.
32. R. Yazami, P. Touzain, *J. Power Sources*, 9 (1983) 365.